

Beyond Invariance: Test-Time Label-Shift Adaptation for Distributions with “Spurious” Correlations

Qingyao Sun University of Chicago	Kevin Murphy Google Brain	Sayna Ebrahimi Google Cloud	Alexander D’Amour Google Brain
--------------------------------------	------------------------------	--------------------------------	-----------------------------------

November 29, 2022

Abstract

Spurious correlations, or correlations that change across domains where a model can be deployed, present significant challenges to real-world applications of machine learning models. However, such correlations are not always “spurious”; often, they provide valuable prior information for a prediction beyond what can be extracted from the input alone. Here, we present a test-time adaptation method that exploits the spurious correlation phenomenon, in contrast to recent approaches that attempt to eliminate spurious correlations through invariance. We consider situations where the prior distribution $p(y, z)$, which models the marginal dependence between the class label y and the nuisance factors z , may change across domains, but the generative model for features $p(\mathbf{x}|y, z)$ is constant. We note that this is an expanded version of the label shift assumption, where the labels now also include the nuisance factors z . Based on this observation, we train a classifier to predict $p(y, z|\mathbf{x})$ on the source distribution, and implement a test-time label shift correction that adapts to changes in the marginal distribution $p(y, z)$ using unlabeled samples from the target domain. We call our method “Test-Time Label-Shift Adaptation” or TTLSA. We apply our method to two different image datasets – the CheXpert chest X-ray dataset and the colored MNIST dataset – and show that it gives better downstream results than methods that try to train classifiers which are invariant to the changes in prior distribution. Code reproducing experiments is available at <https://github.com/nalzok/test-time-label-shift>.

1 Introduction

Classification systems, especially ones based on deep neural networks, are known to be sensitive to “spurious correlations” [Gei+20; Wil+22] between irrelevant features of the inputs (known as the nuisance factors) and the predicted output label. This reduces their performance when they are deployed on a different distribution (known as the *target* domain) from the one used during training (known as the *source* domain, as shown in e.g., [Gei+20; Izm+22]). For example, [Zec+18] found that a convolutional neural network (CNN) trained to recognize pneumonia was relying on hospital-specific metal tokens in the chest X-ray scans (i.e., spurious features in the image background), rather than focusing on the lungs themselves (relevant features in the foreground); this meant that the model did not generalize (or, to use the terminology of [PB14], did not “transport”) to new hospitals.

One way to formalize this problem is to describe the domain in terms of three sets of variables: the observed features X , the observed labels Y , and the other causes of the features, Z . We assume that the relationship between Y and Z is modeled by a set of latent confounding factors U , as shown in Figure 1. We assume that the confounders can change from source to target distribution, and hence $p_t(y, z) \neq p_s(y, z)$; however, we assume that the generative model of the observed data, $p(\mathbf{x}|y, z)$, is stable across domain; this is an expanded version of the label shift or target shift assumption [Zha+13; WV22]. For example, in the case of medical X-ray classification, $\mathbf{x} \in X$ represents the image, $y \in Y$ represents the disease, and $z \in Z$ may correspond to patient attributes like age and sex, or the identity of the hospital used to collect the data; the distribution over disease and attributes may change between populations, but we assume that the mechanism of image generation is stable across domains. See Section 4.1 for more details on this application.

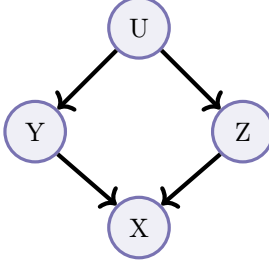


Figure 1: Modeling assumptions. U represents a hidden confounder that induces a spurious correlation between the label Y and other causal factors Z , which together generate the features X .

Several papers attempt to learn classifiers that are *invariant* to changes in Z , such as [Vei+21; Mak+22; Pul+22]. Our approach acknowledges that information in Z is relevant for predicting Y from X (e.g., age is an important factor in interpreting an X-ray). Thus, instead of imposing an artificial invariance on the predictive distribution $p_t(y|\mathbf{x})$, we leverage the true invariance of $p_t(\mathbf{x}|y, z) = p_s(\mathbf{x}|y, z)$ to derive a simple adjustment that yields optimal predictions when the marginal “backdoor” correlation between Y and Z changes. Thus, we expect our method to yield better predictions on the downstream task compared to robustifying methods, especially in cases where the marginal correlation between Y and Z is strong relative to the signal in X , and in cases where Y and Z have a strong interaction in producing the input X .

It is worth noting that although the model in Figure 1 assumes that Z and Y generate the features X (a so-called “anti-causal” model [Sch+12]), our algorithm does not need to learn a generative model of the form $p(\mathbf{x}|y, z)$, but can instead use discriminative classifiers of the form $p(y, z|\mathbf{x})$ to perform the unlabeled adaptation. In more detail, our method works as follows. We assume access to labeled samples from the source distribution, $D_s^{xyz} \sim p_s(\mathbf{x}, y, z)$, which we use to learn the classifier $p_s(y, z|\mathbf{x})$ and prior $p_s(y, z)$, where $y \in \mathcal{Y} = \{1, \dots, C\}$ is the class label, and $z \in \mathcal{Z} = \{1, \dots, K\}$ is the auxiliary label. Given this information, we can derive the likelihood $p_s(\mathbf{x}|y, z)$, as explained in Section 3. At test time, we assume access to unlabeled data from the target distribution, $D_t^x \sim p_t(\mathbf{x})$. We then use the EM algorithm to estimate $p_t(y, z)$ from D_t^x (see Section 3). Finally, we combine this new prior with the likelihood $p(\mathbf{x}|y, z)$ to compute the posterior $p_t(y, z|\mathbf{x})$, from which we can get the label posterior $p_t(y|\mathbf{x})$ by marginalization. We call this procedure “test-time label-shift adaptation” or TTLSA.

We experimentally compare our method to an optimal method for training invariant predictors, and several other baselines, and show that our adaptive scheme works better on two distinct image classification datasets.

2 Related work

Unsupervised Domain Adaptation (UDA) UDA methods attempt to reduce the negative effect of distribution shifts by training a joint model on the labeled source and the unlabeled target data. Some prior works do so using feature alignment techniques [Pen+19; Lon+15; Tze+14] or reconstructing source and target data using autoencoders [Ghi+16] or cycle-consistency GANs [Hof+18]. Adversarial learning based UDA methods also use adversarial two-player games to disentangle domain invariant and domain specific features [GL15; Lon+18; Shu+18]. Self-training based methods use the source domain classifier to create pseudo labels for adaptation [Mei+20; Zha+21; HDV22]. Note that all UDA approaches need to access both labeled source data and unlabeled target data during training, which is a special case for the more challenging setting of test-time adaptation discussed below.

Test Time Adaptation (TTA) using discriminative models TTA is a more general and challenging problem compared to UDA because adaptation is performed using the source model and unlabeled target data, as opposed to having access to both source and target data at the same time. In particular, the approach is

train the classifier on $\mathcal{D}_s^{xy} \sim p_s$ and then adapt it using $\mathcal{D}_t^x \sim p_t^x$ so that it predicts reliably on $\mathcal{D}_t^{xy} \sim p_t^{xy}$. TTA requires some kind of unsupervised cost function. TENT [Wan+21] uses entropy minimization to update the batch normalization layers. However, it is prone to error accumulation when predictions are miscalibrated. SHOT [LHF20] uses clustering-based pseudo labeling along with information maximization. MEMO [ZLF21] uses ensembles of predictions for different augmentations of a test sample. AdaContrast [Che+22] utilizes contrastive self-supervised learning jointly with online pseudo labeling.

Overall, the current literature on TTA has mainly focused on adapting neural networks that work on images (e.g., by leveraging data augmentation), rather than embeddings or other forms of input. It is also not clear how to extend these methods beyond neural networks. In addition, most UDA/TTA papers focus on covariate shift, where $p(x)$ changes, whereas we focus on the anti-causal setting, where the shift is due to a change in the prior over latent factors and/or labels, $p(z, y)$.

Classifiers that are invariant to changes in nuisance variables Several papers attempt to learn classifiers that are *invariant* to changes in Z , such as [Vei+21; Mak+22; Pul+22; ZM22]. These methods partition the features X into those that depend on Z , denoted X_Z , and those that are independent of Z , denoted X_Z^\perp . They then try to learn a predictor for Y that only depends on X_Z^\perp , by training a classifier with additional regularizers that encourage the desired conditional independence. However, enforcing independence in high-dimensional feature spaces is hard. A related line of work tries to minimize the worst-case loss across groups (values for Z) using distributionally robust optimization (see e.g, [Sag+20; Liu+21; Nam+22; Lok+22]). However, both the invariance and group robustness approaches discard potentially useful information in Z . By contrast, we propose to leverage information in Z by adapting to the shift.

Methods using the expanded label shift assumption A similar approach to ours, known as “generative multi-task learning” or GMTL, was recently proposed in [MGC22]. However, instead of estimating $p_t(y, z)$ from unsupervised target data, they instead assume there exists some α such that $p_t(y, z) = p_s(y, z)^{1-\alpha}$. They state that choosing α is an open problem, and therefore they report results for a range of possible α ’s. We show that this gives inferior results compared to our approach, even with the optimal choice of α . In [JV22], they propose a method called Anti-Causal Transportable and Invariant Representation or “ACTIR”, which relaxes the assumption that Z is observed. Instead, they assume access to examples from multiple source distributions, \mathcal{D}_e^{xy} , which they use to learn a domain invariant classifier; they then rapidly adapt this to the target distribution using labeled examples of the form \mathcal{D}_t^{xy} .

3 Method

Our goal is to compute the target distribution over class labels, which is given by

$$p_t(y|\mathbf{x}) = \sum_z p_t(y, z|\mathbf{x}) \tag{1}$$

where $y \in \{1, \dots, C\}$ is the class label of interest, and $z \in \{1, \dots, K\}$ is a “nuisance variable”. By Bayes rule, we have

$$p_t(y, z|\mathbf{x}) = p_t(m|\mathbf{x}) = \frac{p_t(\mathbf{x}|m)p_t(m)}{p_t(\mathbf{x})} \tag{2}$$

where we have defined $m = y \times K + z$, such that each value of $m \in \{1, \dots, M\}$, where $M = C \times K$, corresponds to a unique pair of (y, z) .

By the label shift assumption, this becomes

$$p_t(m|\mathbf{x}) = \frac{p_s(\mathbf{x}|m)p_t(m)}{\sum_{m'} p_s(\mathbf{x}|m')p_t(m')} \tag{3}$$

where $p_s(\mathbf{x}, y, z)$ is the source distribution, and $p_t(\mathbf{x}, y, z)$ is the target distribution. Computing Equation (3) seems to require a generative model $p_s(\mathbf{x}|m)$. However, we can use the scaled likelihood trick [Ren+94] to

rewrite the class-conditional generative model $p_s(\mathbf{x}|m)$ in terms of a discriminative classifier $p_s(m|\mathbf{x})$ and source label prior $p_s(m)$:

$$p_s(\mathbf{x}|m) = \frac{p_s(m|\mathbf{x})p_s(\mathbf{x})}{p_s(m)} = C \frac{p_s(m|\mathbf{x})}{p_s(m)} \quad (4)$$

where the constant $C = p_s(\mathbf{x})$ is independent of m . Hence the target classifier is given by

$$p_t(m|\mathbf{x}) = \frac{w(m)p_s(m|\mathbf{x})}{\sum_{m'=1}^M w(m')p_s(m'|\mathbf{x})} \quad (5)$$

where $w(m) = \frac{p_t(m)}{p_s(m)}$. Hence all we have to do is to estimate the discriminative model $p_s(m|\mathbf{x})$ and the label prior $p_s(m)$ on the labeled source distribution, and then estimate the shifted label prior $p_t(m)$ on the unlabeled target distribution. We give the details below.

Step 1: Fit model on the source distribution

First we train a discriminative classifier to predict the combined label using $p_s(m|\mathbf{x})$ which we fit to \mathcal{D}_s^{xyz} . Then we calibrate this classifier using a labeled validation set (a subset of \mathcal{D}_s^{xyz}). This step is important since [Guo+17] has shown modern neural networks are poorly calibrated. In [AKS20] they propose “bias corrected temperature scaling” (BCTS), which is a generalization of Platt scaling to the multi-class case. In particular, let $l(\mathbf{x})$ be the vector of M logits. We then modify $p_s(m|\mathbf{x})$ as follows:

$$p_s(m|\mathbf{x}) = \frac{\exp(l(\mathbf{x})_m/T + b_m)}{\sum_{m'=1}^M \exp(l(\mathbf{x})_{m'}/T + b_{m'})} \quad (6)$$

where $T \geq 0$ is a learned temperature parameter, and b_m is a learned bias.

We could estimate the source label prior, $p_s(m)$, from the empirical counts on \mathcal{D}_s^{xyz} , but [AKS20] argue that it is better to compute the label prior induced by the classifier’s output:

$$p_s(m) = \frac{1}{N} \sum_{n \in \mathcal{D}_s^{xyz}} p_s(m|\mathbf{x}_n) \quad (7)$$

Step 2: Adapt model to the target distribution

Next we estimate the label prior on the target distribution, $p_t(y, z) = p_t(m) = \boldsymbol{\pi}_m$, using the unlabeled data \mathcal{D}_t^x . There are several approaches to this, including a moment matching method called black box shift learning [LWS18] and an MLE approach based on the EM algorithm [SLD02]. In [AKS20], they show that the MLE approach is much better, provided the classifier is calibrated. (See also [Gar+20] for a unified analysis of these two approaches.)

Since our augmented label space is expanded to include both class labels y and meta-data z , the number of labels M can be large, which can result in problems when computing the MLE. We therefore expand the previous approach to compute the MAP estimate, using a Dirichlet prior of the form

$$\text{Dir}(\boldsymbol{\pi}|\boldsymbol{\alpha}) = \frac{1}{B(\boldsymbol{\alpha})} \prod_{m=1}^M \boldsymbol{\pi}_m^{\alpha_m-1} \quad (8)$$

where $B(\boldsymbol{\alpha})$ is the normalization constant. Note that the MLE solution can be recovered by setting $\boldsymbol{\alpha} = \mathbf{1}$, which represents a uniform prior.

The goal is to maximize the (unnormalized) log posterior of $\boldsymbol{\pi}$ given the unlabeled target data \mathbf{X} :

$$\mathcal{L}(\mathbf{X}; \boldsymbol{\pi}) = \log p_t(\boldsymbol{\pi}, \mathbf{X}) \quad (9)$$

$$= \log p_t(\mathbf{X}|\boldsymbol{\pi}) + \log \text{Dir}(\boldsymbol{\pi}|\boldsymbol{\alpha}) \quad (10)$$

$$= \sum_{n=1}^N \log p_t(\mathbf{x}_n|\boldsymbol{\pi}) + \log \text{Dir}(\boldsymbol{\pi}|\boldsymbol{\alpha}) \quad (11)$$

$$= \sum_{n=1}^N \log \left[\sum_{m=1}^M \boldsymbol{\pi}_m p_t(\mathbf{x}_n|m) \right] + \log \text{Dir}(\boldsymbol{\pi}|\boldsymbol{\alpha}) \quad (12)$$

The first term can be rewritten as

$$\sum_n \log \left[\sum_{m=1}^M \boldsymbol{\pi}_m p_s(\mathbf{x}_n|m) \right] = \sum_n \log \left[\sum_{m=1}^M \boldsymbol{\pi}_m \frac{p_s(m|\mathbf{x}_n) p_s(\mathbf{x}_n)}{p_s(m)} \right] \quad (13)$$

$$= \sum_n \log \sum_m \frac{p_s(m|\mathbf{x}_n)}{p_s(m)} \boldsymbol{\pi}_m + \text{const} \quad (14)$$

This objective is a sum of logs of a linear function of $\boldsymbol{\pi}$, as is the log prior. This needs to be maximized subject to the affine constraints $\boldsymbol{\pi}_m \geq 0$ and $\sum_{m=1}^M \boldsymbol{\pi}_m = 1$, so the problem is concave, with a unique global optimum [AKS20].

One way to compute this optimum is to use EM. Let $\boldsymbol{\pi}^j$ be the estimate of $\boldsymbol{\pi}$ at iteration j ; we initialize with $\boldsymbol{\pi}_m^0 = p_s(m)$. First note that

$$p_t(\mathbf{x}_n, m_n) = p_s(\mathbf{x}_n|m_n) p_t(m_n) = \prod_{m=1}^M [p_s(\mathbf{x}_n|m) \boldsymbol{\pi}(m)]^{\mathbb{I}(m_n=m)} \quad (15)$$

Hence the complete data log posterior is given by

$$\mathcal{L}(\mathbf{X}, \mathbf{M}; \boldsymbol{\pi}) = \sum_{n=1}^N \sum_{m=1}^M \mathbb{I}(m_n=m) \log[\boldsymbol{\pi}_m p_s(\mathbf{x}_n|m)] + \log \text{Dir}(\boldsymbol{\pi}|\boldsymbol{\alpha}) \quad (16)$$

so the expected complete data log posterior is

$$Q(\boldsymbol{\pi}, \boldsymbol{\pi}^{(j)}) = E_{\mathbf{M}}[\mathcal{L}(\mathbf{X}, \mathbf{M}; \boldsymbol{\pi}) | \mathbf{X}, \boldsymbol{\pi}^{(j)}] \quad (17)$$

$$= \sum_{n=1}^N \sum_{m=1}^M p(m_n=m|\mathbf{X}, \boldsymbol{\pi}^{(j)}) \log(\boldsymbol{\pi}_m p_s(\mathbf{x}_n|m)) + \log \text{Dir}(\boldsymbol{\pi}|\boldsymbol{\alpha}) \quad (18)$$

$$= \sum_{m=1}^M N_m^j \log(\boldsymbol{\pi}_m p_s(\mathbf{x}_n|m)) + \sum_{m=1}^M (\alpha_m - 1) \log \boldsymbol{\pi}_m - \log B(\boldsymbol{\alpha}) \quad (19)$$

$$= \sum_{m=1}^M N_m^j \log \boldsymbol{\pi}_m + \underbrace{\sum_{m=1}^M N_m^j \log p_s(\mathbf{x}_n|m)}_{\text{const}} + \sum_{m=1}^M (\alpha_m - 1) \log \boldsymbol{\pi}_m + \text{const} \quad (20)$$

where we drop constants wrt $\boldsymbol{\pi}$, and where we defined the expected counts to be

$$N_m^j = \sum_{n=1}^N p(m_n=m|\mathbf{x}_n, \boldsymbol{\pi}^{(j)}) \quad (21)$$

Hence in the E step we just need to compute the posterior responsibilities for each label:

$$p(m_n = m | \mathbf{x}_n, \boldsymbol{\pi}^j) = \frac{\boldsymbol{\pi}^j(m) p_s(\mathbf{x}_n | m)}{\sum_{m'=1}^M \boldsymbol{\pi}^j(m') p_s(\mathbf{x}_n | m')} = \frac{\boldsymbol{\pi}^j(m) p_s(m | \mathbf{x}_n) / p_s(m)}{\sum_{m'=1}^M \boldsymbol{\pi}^j(m') p_s(m' | \mathbf{x}_n) / p_s(m')} \quad (22)$$

We plug this into Equation (21) and then maximize Equation (20), using a Lagrange multiplier to enforce the sum to one constraint. We then get the following (see e.g., Sec 4.2.4 of [Mur22] for the derivation):

$$\hat{\boldsymbol{\pi}}_m^{j+1} = \frac{\tilde{N}_m^j}{\sum_{m'=1}^M \tilde{N}_{m'}^j} \quad (23)$$

where \tilde{N}_m^j are the prior pseudo counts plus the expected empirical counts:

$$\tilde{N}_m^j = N_m^j + \alpha_m - 1 \quad (24)$$

At convergence, we have

$$p_t(y, z) = \hat{\boldsymbol{\pi}}_{y,z}^J \quad (25)$$

If we assume that the class label prior is constant, and only the distribution of auxiliary labels has changed, then we can write

$$p_t(y, z) = p_s(y) p_t(z | y) \quad (26)$$

where

$$p_t(z | y) = \frac{p_t(y, z)}{\sum_{z'} p_t(y, z')} \quad (27)$$

However, we do not make this fixed label assumption in our experiments.

4 Experiments

In this section, we provide an experimental comparison of our method on two different datasets: the CheXpert chest X-ray dataset discussed in Section 4.1, and a ColoredMNIST discussed in Section 4.2. In both cases, we create a set of 21 distributions $p_\lambda = (1 - \lambda)p_0 + \lambda p_1$, where $\lambda \in \{0, 0.05, \dots, 0.95, 1.0\}$, and $p_0(y, z)$ and $p_1(y, z)$ are two anchor distributions in which y and z are correlated and anti-correlated, respectively. By changing λ , we can control the dependence between y and z .

We consider the following baseline methods:

Unadapted This corresponds to training a model on the source distribution, and then applying the same model to the target distribution without any adaptation, i.e., we assume $p_t(\mathbf{x}|y, z) = p_s(\mathbf{x}|y, z)$.

Oracle This corresponds to making predictions on the target distribution using the true (but unobservable) label prior $p_t(y, z)$, together with the learned probability $p_s(y, z | \mathbf{x})$. In other words, we calculate $p_t(\mathbf{x}|y, z)$ using Equation 5 assuming oracle access to $p_t(y, z)$.

GMLT This corresponds to the recent ‘‘generative multi-task learning’’ approach of [MGC22], which is equivalent to assuming $p_t(y, z) \propto p_s(y, z)^{1-\alpha}$. We follow their approach of reporting results for a range of possible α ’s¹.

Invariant This is an approximation to the best possible risk invariant predictor; we discuss how to compute this below.

¹We relax the constraint $0 \leq \alpha \leq 1$ and allow $\alpha \in \mathbb{R}$ instead.

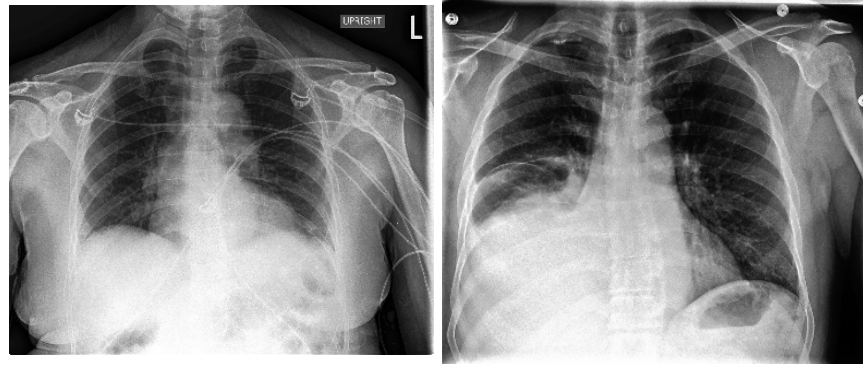


Figure 2: Samples from CheXpert. **Left:** Female patient without effusion. **Right:** Male patient with effusion.

To approximate the optimal risk invariant predictor, we take inspiration from Proposition 1 of [Mak+22], which showed that a classifier that is trained on the independent distribution $p(y, z) = p(y)p(z)$ will not learn any “shortcut” between the confounding factor z and the target label y . Such a model will therefore have a risk which is invariant to changes in the $p(y, z)$ distribution, and they showed that this is indeed the optimal one among all risk-invariant predictors. We can simulate this optimal predictor by training it on an unconfounded distribution with $p(y, z) = p(y)p(z)$; this corresponds to training on the distribution with $\lambda = 0.5$.

Having trained our classifiers with these methods, we then evaluate them on fresh samples from p_λ for $\lambda \in \{0, 0.05, \dots, 0.95, 1.0\}$. We measure performance using Area Under the ROC curve (AUC); this is a better metric than classification accuracy, since several datasets have very skewed label priors (see e.g. Table 1), which means the base rate accuracy can already be very high.

We show that our method (denoted EM) comes close to the oracle performance, and outperforms Unadapted, GMTL, and Invariant. Our code is open-sourced at <https://github.com/nalzok/test-time-label-shift>.

4.1 CheXpert

In this section, we apply our method to the problem of disease classification using chest X-rays based on the CheXpert [Irv+19] dataset.

4.1.1 Dataset

CheXpert has 224,316 chest radiographs of 65,240 patients. Each image is associated with 14 disease labels derived from radiology reports, and 3 potentially confounding attributes (age, sex, and race), as listed in Table 1. We binarized the attributes as in [Jab+20], taking age to be 0 if below the median and 1 if above, and sex to be 0 if female and 1 if male. As for the class labels, we define class 0 as “negative” (corresponding to no evidence of a disease), and class 1 as “positive” (representing the presence of a disease); images labeled “uncertain” for the attribute of interest are discarded. Following [Glo+22], we focus on predicting the label $y = \text{“Pleural Effusion”}$ and use sex as the confounding variable z . See Figure 2 for some samples from the dataset.

For the input features \mathbf{x} , we consider two setups. The first setup works with the raw gray-scale images, rescaled to size 224×224 . The second setup uses 1376-dim feature embeddings derived from the pretrained CXR model [Sel+22]. This embedding model was pre-trained on a large set of weakly labeled X-rays from the USA and India. Note, however, that the pre-training dataset for CXR is distinct from the CheXpert dataset we use in our experiments.

		z		z	
		0	1	0	1
		0	0.5	0	0.5
y	0	0.5	0	0	0.5
	1	0	0.5	0.5	0

Table 2: The two “anchor” distributions, reflecting total positive and negative correlation between the class label y and the confounding factor z . Left: p_0 . Right: p_1 .

Attribute	AUC	Mean
NO_FINDING	0.873	0.909
ENLARGED_CARDIOMEDIASTINUM	0.652	0.942
CARDIOMEGLY	0.843	0.867
AIRSPACE_OPACITY	0.711	0.480
LUNG_LESION	0.761	0.963
PULMONARY_EDEMA	0.848	0.696
CONSOLIDATION	0.683	0.911
PNEUMONIA	0.742	0.973
ATELECTASIS	0.694	0.815
PNEUMOTHORAX	0.883	0.875
EFFUSION	0.861	0.508
PLEURAL_OTHER	0.752	0.987
FRACTURE	0.784	0.962
SUPPORT_DEVICES	0.900	0.420
GENDER	0.973	0.586
AGE_AT_CXR	0.914	0.492
PRIMARY_RACE	0.731	0.459
ETHNICITY	0.681	0.728

Table 1: Metrics for all the attributes in the CheXpert dataset. (a) AUC using Logistic Regression on CXR embeddings. (b) Baseline prior probability for each attribute, illustrating the severe class imbalance for many attributes.

When working with embeddings, we use a simple linear logistic regression model, following [Sel+22], due to its simplicity and its reasonable performance. To verify this, we train a classifier to predict all the attributes, using an 80/20 split of the CheXpert embeddings; for the optimizer we used Adam with a learning rate 10^{-3} for 1000 epochs. The resulting AUC scores are shown in Table 1. This shows we can reliably predict all the attributes from the embeddings. For example, we see that we can predict sex with an AUC of 0.973. This is higher than the AUC for effusion, which is just 0.861. To understand why, note that we only use frontal scans; consequently breasts are often visible in female patients, and this is often easier to detect visually than detecting the disease itself (see Figure 2), providing a possible “shortcut” for models to exploit. Table 1 also shows the marginal distribution of each attribute. Many labels are highly skewed, which means accuracy would be a poor measure of the predictive performance.

To compare performance under distribution shift, we created a set of 21 distributions, $p_\lambda = (1 - \lambda)p_0 + \lambda p_1$, where $\lambda \in \{0, 0.05, \dots, 0.95, 1.0\}$ interpolates between two anchor distributions: in p_0 we have $z \stackrel{a.s.}{=} y$ and in p_1 , we have $z \neq y$, with uniform marginals, as shown in Table 2. For the training distribution, we use $\lambda = 0.5$ and $\lambda = 0.1$, and for the test distributions, we use all 21 values of λ . The test images are distinct from the training, and each test distribution has 512 samples in total. Each patient may have multiple images associated with them, but there is no patient overlap in the training and test distributions.

4.1.2 Model

We train a classifier to predict $m = (y, z)$ given inputs \mathbf{x} . When working with raw images, we use a ResNet-50 CNN pretrained on the ImageNet dataset. In particular, we modify our gray-scale input to match the ImageNet model by replicating the image along the RGB channels in the input layer. We use AdamW with a batch size of 64 and a learning rate of 10^{-3} for 100 epochs, and run calibration for 20 epochs with the same learning rate and batch size on a 10% holdout set. During evaluation, we infer the target label prior for each target distribution using EM applied to an unlabeled test set of size 64 or 512. For the source prior, we choose $\alpha_m = M \times p_s(m)$ to regularize $\hat{p}_t(m)$ towards $p_s(m)$. We then predict the class labels for that same test dataset.

When working with embeddings, we use a simple linear logistic regression model. We use AdamW with a batch size of 64 and a learning rate of 10^{-3} for 500 epochs, and run calibration for 100 epochs with the same learning rate and batch size on a 10% holdout set. Not only is this faster to train than a CNN applied to pixels, but it also gives better results (compare Figure 3 to Figure 4), as was previously shown in [Sel+22]. Evaluation is performed in the same way as predicting with raw pixels.

To emphasize that our method can also be applied to non-neural net classifiers, we show our method using gradient boosting models applied to the embeddings. Specifically, we use `HistGradientBoostingClassifier` from scikit-learn [Ped+11] with default parameters. For simplicity, we did not run calibration on gradient boosting models, and adapted on all samples in the target domain instead of doing adaptation in batches.

4.1.3 Results

In Figure 3a, we show the results of each method when the classifier $p(y, z|\mathbf{x})$ is trained on the unconfounded distribution with $\lambda = 0.5$, where $p(y, z) = p(y)p(z)$ is the uniform distribution. The horizontal light gray line shows the results of applying this unadapted classifier to each of the test distributions; we see that the performance is constant, as expected. The horizontal blue lines show the results of GMTL for $\alpha \in \{0.5, 1.0, 2.0\}$; these are all equivalent to the unadapted model in this case, since the source distribution is uniform. The U-shaped dotted black line shows the results of the oracle method, which combines the learned classifier with the true prior $p_t(y, z)$ for each test distribution; this is an upper bound on performance. Finally, the yellow and orange curves show the result of our EM method, where we estimate the target prior using either $N = 64$ or $N = 512$ examples. We see that the EM method closely tracks the oracle method, with performance being better for larger N . Importantly, we see that the adaptive methods (oracle and EM) outperform the invariant methods.

In Figure 3b, we show the results of each method when the classifier $p(y, z|\mathbf{x})$ is trained on the confounded distribution with $\lambda = 0.1$. Now the difference in behavior of the methods becomes more apparent. The light gray line shows that the performance of the unadapted model gets steadily worse as the target distribution moves further away from the source distribution (the curve goes down and to the right). The classifier trained on $\lambda = 0.5$, which emulates an invariant classifier, has constant performance (see horizontal green line), as before. Once again, EM (orange and red) closely tracks the oracle performance (black), which outperforms the invariant method.

Finally, we see that the behavior of GMTL (blue) depends on α . It has good performance if and only if the label distribution generated by α is close to the ground truth. In particular, when training on the confounded distribution (Figure 7b), the target label distribution has an opposite correlation to the source domain when $\alpha > 1$, so the GMTL curve with $\alpha = 2$ performs poorly when λ is close to 0, but its AUC can be as good as oracle when λ is close to 1.

In Figure 4 we show the results when we use a CNN applied to raw pixels, rather than using logistic regression applied to the embeddings. The trends are the same as before, although absolute performance is somewhat lower. Finally, in Figure 5, we show the results with gradient boosting applied to the embeddings. We see that the trend is similar to using logistic regression, demonstrating the versatility of our method.

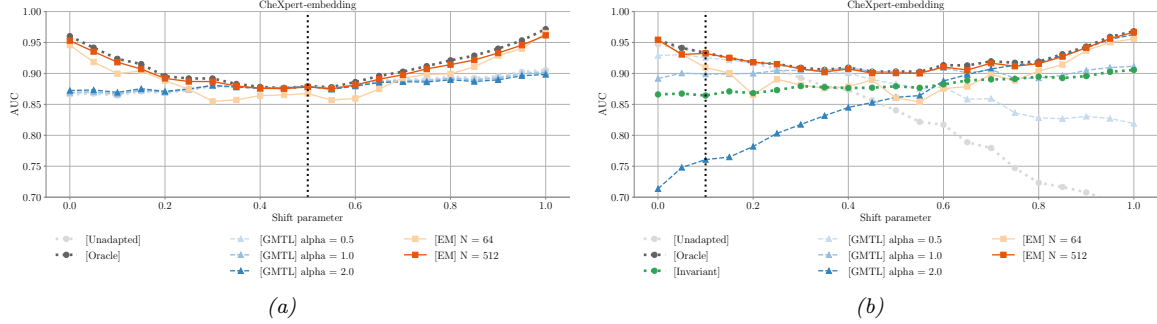


Figure 3: Results using logistic regression on CheXpert embeddings. (a) Classifier is trained on unconfounded distribution, $\lambda = 0.5$. (b) Classifier is trained on confounded distribution, $\lambda = 0.1$.

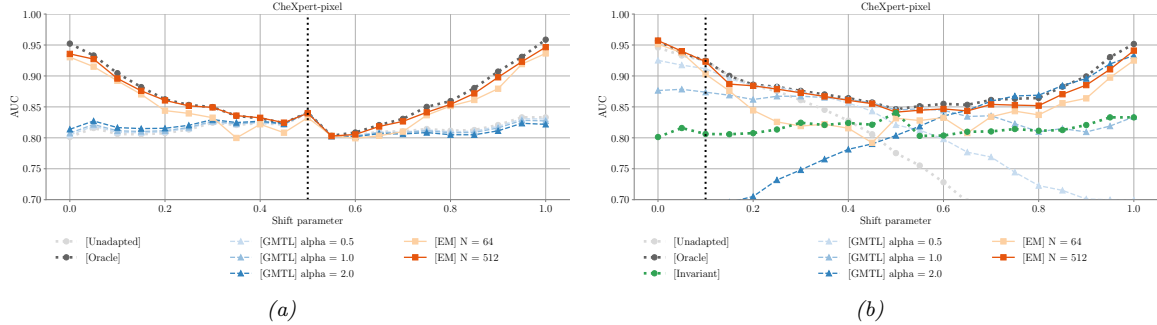


Figure 4: Results using ResNet-50 CNNs on CheXpert images. (a) Classifier is trained on unconfounded distribution, $\lambda = 0.5$. (b) Classifier is trained on confounded distribution, $\lambda = 0.1$.

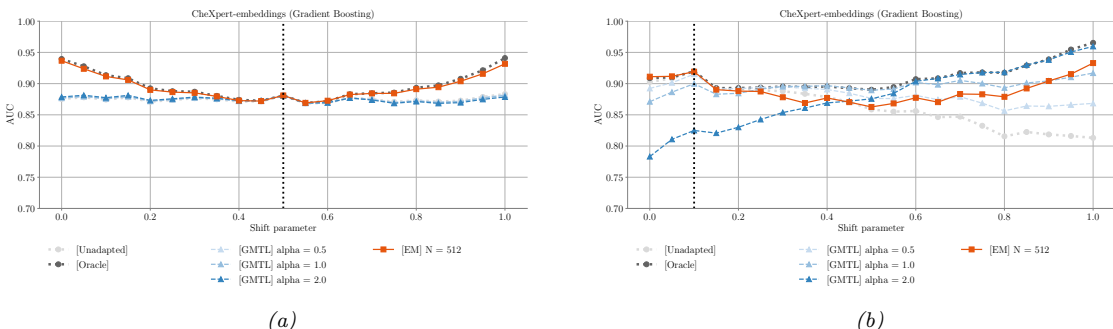


Figure 5: Results using gradient boosting models on CheXpert embeddings. (a) Classifier is trained on unconfounded distribution, $\lambda = 0.5$. (b) Classifier is trained on confounded distribution, $\lambda = 0.1$.



Figure 6: Samples from ColoredMNIST. (a): $y = 1, z = 0$. (b) $y = 1, z = 1$.

4.1.4 Discussion

In [Glo+22], they point out that embeddings derived from X-ray classification models may contain information about “sensitive attributes” Z , such as sex and age. We confirmed this result, and were able to classify sex with an accuracy of over 95% just using logistic regression on the CXR embeddings, as shown in Table 1. In [Glo+22], they argue that this may be harmful, since it can cause bias in the predictions of the primary label Y of interest (disease status). However, our results show that we can predict both Z and Y from the embeddings and then use Z as an additional feature to predict Y . This gives us improved performance on downstream applications, and could result in *increased* fairness (c.f., [MD22]).

4.2 ColoredMNIST

In this section, we apply our method to the ColoredMNIST dataset constructed in a manner similar to [Arj+19] and [GL21].

4.2.1 Dataset

We construct 21 domains from MNIST by transforming each example as follows: first, we assign a preliminary binary label \tilde{y} to the image based on the digit: $\tilde{y} = 0$ for digits 0-4 and $\tilde{y} = 1$ for 5-9. Second, we obtain the observed noisy label y by flipping \tilde{y} with a probability of $\phi = 0.1$. (We add noise to the labels, since otherwise Y can be perfectly predicted from X .) Third, we sample the color $z = 1$ with probability $\frac{1}{20}i$ for the i th domain, where $z = 1$ corresponds to red and $z = 0$ corresponds to green. See Figure 6 for some samples from the dataset.

Formally, the joint distribution of (\tilde{y}, y) is

$$p_i(\tilde{y}, y) = \begin{array}{c|cc} \tilde{y} \backslash y & 0 & 1 \\ \hline 0 & 1 - \phi & \phi \\ 1 & \phi & 1 - \phi \end{array} \quad (28)$$

and the joint distribution of (y, z_{col}) in the i th domain is

$$p_i(y, z_{\text{col}}) = \begin{array}{c|cc} y \backslash z_{\text{col}} & 0 (\text{red}) & 1 (\text{green}) \\ \hline 0 & \frac{1}{2}(1 - \rho_i) & \frac{1}{2}\rho_i \\ 1 & \frac{1}{2}\rho_i & \frac{1}{2}(1 - \rho_i) \end{array} \quad (29)$$

where $\rho_i = \frac{1}{20}i$.

We define $p(\mathbf{x}|z, y)$ as follows. We first split the data into two halves, \mathcal{X}_s and \mathcal{X}_t ; we then define $\mathcal{X}_s(y, z) = \{\mathbf{x}_n \in \mathcal{X}_s : z_n = z, y_n = y\}$ to be the set of source images with the specified pair of labels; we define $\mathcal{X}_t(y, z)$ similarly. Finally we define $p_s(\mathbf{x}, y, z) = p_s(y, z)\text{Unif}(\mathcal{X}_s(y, z))$; this means we generate a

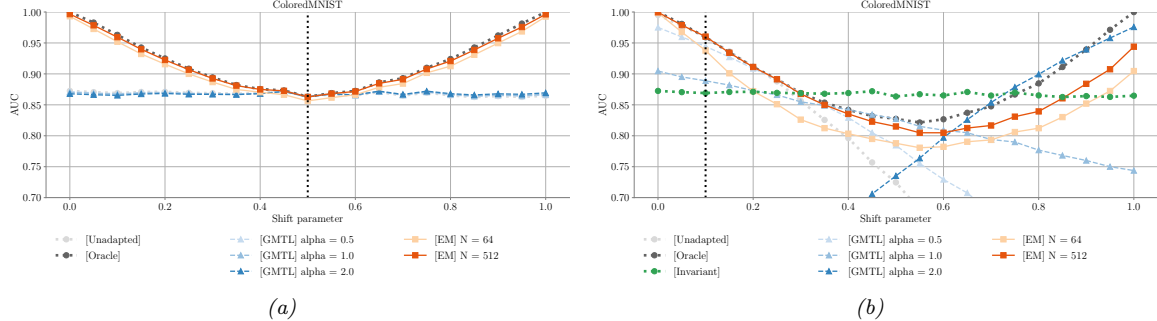


Figure 7: Results using LeNet CNNs on ColoredMNIST. (a) Classifier is trained on unconfounded distribution, $\lambda = 0.5$. (b) Classifier is trained on confounded distribution, $\lambda = 0.1$.

source example as follows: first sample a label pair (y, z) from p_s , then pick an image with that label pair uniformly at random from the training images, $\mathcal{X}_s(y, z)$. We define $p_t^i(\mathbf{x}, y, z) = p_i(y, z)\text{Unif}(\mathcal{X}_t(y, z))$ for the i 'th target distribution in a similar way.

4.2.2 Training procedure

During training, we fit a LeNet CNN on the training set by using $m = (y, z)$ as the label. We use AdamW with a batch size of 64 and a learning rate of 10^{-3} for 500 epochs, and run calibration for 100 epochs with the same learning rate and batch size on a 10% holdout set. We also fit a gradient boosted classifier to the pixels.

During evaluation, we infer the target label prior for each target distribution using EM applied to an unlabeled test set of size 64 or 512. For the source prior, we choose $\alpha_m = M \times p_s(m)$ to regularize $\hat{p}_t(m)$ towards $p_s(m)$. We then predict the class labels for that same test dataset.

4.2.3 Results

Figure 7 shows our results using a CNN, and Figure 8 shows our results using gradient boosting. Here are the key takeaways:

- As in CheXpert, our EM algorithm closely matches the oracle method, with a larger test set size ($N = 512$) giving better results.
- As in CheXpert, the GMTL performance depends on α , and is generally worse than our EM method.
- Surprisingly, the invariant curve (green line) in Figure 7b is higher than the oracle (black line) when λ is close to 0.5. Note, however, that these two classifiers are trained on different datasets (albeit of the same size, namely 28,000 images). In particular, the invariant model is trained on data samples from $p_{0.5}(\mathbf{x}, y, z)$, but all the other models (including the oracle) are trained on data sampled from $p_{0.1}(\mathbf{x}, y, z)$. These differ not only in their label priors, but also in the images that are sampled. Since the invariant training set is more similar to the $\lambda = 0.5$ test set than the oracle training set, it suggests that the model may simply be “overfitting”.

5 Conclusion and Future Work

We have shown that adapting to changes in the nuisance factors Z can give better results than using classifiers that are designed to be robust to such changes. However, one weakness of our approach is that we need access to labeled examples of Z during training. In the future, we would like to relax this assumption, by using semi-supervised methods (c.f, [Soh+21; Lok+22; Nam+22]) that combine small fully labeled datasets,

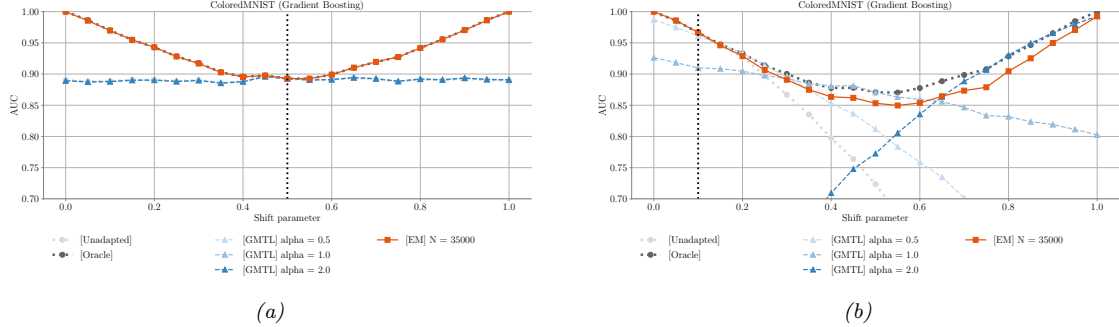


Figure 8: Results using gradient boosting models on ColoredMNIST. (a) Classifier is trained on unconfounded distribution, $\lambda = 0.5$. (b) Classifier is trained on confounded distribution, $\lambda = 0.1$.

\mathcal{D}_s^{xyz} , with large partially labeled datasets, \mathcal{D}_s^{xy} , when training the source classifier.² We also plan to explore the use of fully unsupervised estimates of the confounding factors Z , as well as the use of generative (rather than discriminative) models.

Acknowledgements

We would like to thank Andrew Sellergren for his help with the CheXpert CXR embeddings.

²Although several papers present methods that do not need any access to Z when training the classifier, they still require access to Z labels for hyper-parameter tuning to get good performance (see e.g., Table 2 of [KIW22]).

References

Alexandari, Amr, Anshul Kundaje, and Avanti Shrikumar. “Maximum Likelihood with Bias-Corrected Calibration is Hard-To-Beat at Label Shift Adaptation”. In: *Proceedings of the 37th International Conference on Machine Learning*. Ed. by Hal Daumé III and Aarti Singh. Vol. 119. Proceedings of Machine Learning Research. PMLR, July 2020, pp. 222–232. URL: <https://proceedings.mlr.press/v119/alexandari20a.html>.

Arjovsky, Martin et al. *Invariant Risk Minimization*. 2019. DOI: [10.48550/ARXIV.1907.02893](https://doi.org/10.48550/ARXIV.1907.02893). URL: <https://arxiv.org/abs/1907.02893>.

Chen, Dian et al. “Contrastive Test-Time Adaptation”. In: *CVPR*. 2022, pp. 295–305.

Ganin, Yaroslav and Victor Lempitsky. “Unsupervised domain adaptation by backpropagation”. In: *International conference on machine learning*. PMLR. 2015, pp. 1180–1189.

Garg, Saurabh et al. “A Unified View of Label Shift Estimation”. In: *Advances in Neural Information Processing Systems*. Ed. by H. Larochelle et al. Vol. 33. Curran Associates, Inc., 2020, pp. 3290–3300. URL: <https://proceedings.neurips.cc/paper/2020/file/219e052492f4008818b8adb6366c7ed6-Paper.pdf>.

Geirhos, Robert et al. “Shortcut learning in deep neural networks”. In: *Nature Machine Intelligence* 2.11 (Nov. 2020), pp. 665–673. DOI: [10.1038/s42256-020-00257-z](https://doi.org/10.1038/s42256-020-00257-z). URL: <https://doi.org/10.1038/s42256-020-00257-z>.

Ghifary, Muhammad et al. “Deep reconstruction-classification networks for unsupervised domain adaptation”. In: *European conference on computer vision*. Springer. 2016, pp. 597–613.

Glocker, Ben et al. “Risk of Bias in Chest X-ray Foundation Models”. In: (Sept. 2022). arXiv: [2209.02965 \[cs.LG\]](https://arxiv.org/abs/2209.02965). URL: <http://arxiv.org/abs/2209.02965>.

Gulrajani, Ishaan and David Lopez-Paz. “In Search of Lost Domain Generalization”. In: *International Conference on Learning Representations*. 2021. URL: <https://openreview.net/forum?id=1QdXeDoWtI>.

Guo, Chuan et al. “On calibration of modern neural networks”. In: (2017). arXiv: [1706.04599 \[cs.LG\]](https://arxiv.org/abs/1706.04599).

Hoffman, Judy et al. “CyCADA: Cycle-Consistent Adversarial Domain Adaptation”. In: *Proceedings of the 35th International Conference on Machine Learning*. Ed. by Jennifer Dy and Andreas Krause. Vol. 80. Proceedings of Machine Learning Research. PMLR, July 2018, pp. 1989–1998. URL: <https://proceedings.mlr.press/v80/hoffman18a.html>.

Hoyer, Lukas, Dengxin Dai, and Luc Van Gool. “Daformer: Improving network architectures and training strategies for domain-adaptive semantic segmentation”. In: *Proceedings of the IEEE/CVF Conference on Computer Vision and Pattern Recognition*. 2022, pp. 9924–9935.

Irvin, Jeremy et al. “CheXpert: A Large Chest Radiograph Dataset with Uncertainty Labels and Expert Comparison”. In: *Proceedings of the AAAI Conference on Artificial Intelligence* 33.01 (July 2019), pp. 590–597. DOI: [10.1609/aaai.v33i01.3301590](https://ojs.aaai.org/index.php/AAAI/article/view/3834). URL: <https://ojs.aaai.org/index.php/AAAI/article/view/3834>.

Izmailov, Pavel et al. “On Feature Learning in the Presence of Spurious Correlations”. In: *NIPS*. Oct. 2022. URL: <https://arxiv.org/abs/2210.11369>.

Jabbour, Sarah et al. “Deep Learning Applied to Chest X-Rays: Exploiting and Preventing Shortcuts”. In: *Proceedings of the 5th Machine Learning for Healthcare Conference*. Ed. by Finale Doshi-Velez et al. Vol. 126. Proceedings of Machine Learning Research. PMLR, Aug. 2020, pp. 750–782. URL: <https://proceedings.mlr.press/v126/jabbour20a.html>.

Jiang, Yibo and Victor Veitch. “Invariant and Transportable Representations for Anti-Causal Domain Shifts”. In: (July 2022). arXiv: [2207.01603 \[cs.LG\]](https://arxiv.org/abs/2207.01603). URL: [http://arxiv.org/abs/2207.01603](https://arxiv.org/abs/2207.01603).

Kirichenko, Polina, Pavel Izmailov, and Andrew Gordon Wilson. “Last Layer Re-Training is Sufficient for Robustness to Spurious Correlations”. In: (Apr. 2022). arXiv: [2204.02937 \[cs.LG\]](https://arxiv.org/abs/2204.02937). URL: [http://arxiv.org/abs/2204.02937](https://arxiv.org/abs/2204.02937).

Liang, Jian, Dapeng Hu, and Jiashi Feng. “Do We Really Need to Access the Source Data? Source Hypothesis Transfer for Unsupervised Domain Adaptation”. In: *International Conference on Machine Learning (ICML)*. 2020, pp. 6028–6039.

Lipton, Zachary, Yu-Xiang Wang, and Alexander Smola. "Detecting and Correcting for Label Shift with Black Box Predictors". In: *Proceedings of the 35th International Conference on Machine Learning*. Ed. by Jennifer Dy and Andreas Krause. Vol. 80. Proceedings of Machine Learning Research. PMLR, July 2018, pp. 3122–3130. URL: <https://proceedings.mlr.press/v80/lipton18a.html>.

Liu, Evan Zheran et al. "Just Train Twice: Improving Group Robustness without Training Group Information". In: *ICML*. July 2021. URL: <http://arxiv.org/abs/2107.09044>.

Lokhande, Vishnu Suresh et al. "Towards Group Robustness in the presence of Partial Group Labels". In: *ICML Workshop on Spurious Correlations, Invariance and Stability*. Jan. 2022. URL: <http://arxiv.org/abs/2201.03668>.

Long, Mingsheng et al. "Conditional adversarial domain adaptation". In: *Advances in neural information processing systems* 31 (2018).

Long, Mingsheng et al. "Learning transferable features with deep adaptation networks". In: *International conference on machine learning*. PMLR. 2015, pp. 97–105.

Makar, Maggie and Alexander D'Amour. "Fairness and robustness in anti-causal prediction". In: (Sept. 2022). arXiv: [2209.09423 \[cs.LG\]](2209.09423). URL: <http://arxiv.org/abs/2209.09423>.

Makar, Maggie et al. "Causally motivated shortcut removal using auxiliary labels". In: *AISTATS*. Vol. 151. 2022, pp. 739–766. URL: <https://proceedings.mlr.press/v151/makar22a/makar22a.pdf>.

Makino, Taro, Krzysztof J Geras, and Kyunghyun Cho. "Generative multitask learning mitigates target-causing confounding". In: (Feb. 2022). arXiv: [2202.04136 \[cs.LG\]](2202.04136). URL: <http://arxiv.org/abs/2202.04136>.

Mei, Ke et al. "Instance adaptive self-training for unsupervised domain adaptation". In: *European conference on computer vision*. Springer. 2020, pp. 415–430.

Murphy, K. P. *Probabilistic Machine Learning: An introduction*. MIT Press, 2022.

Nam, Junhyun et al. "Spread Spurious Attribute: Improving Worst-group Accuracy with Spurious Attribute Estimation". In: *ICLR*. Apr. 2022. URL: <http://arxiv.org/abs/2204.02070>.

Pearl, Judea and Elias Bareinboim. "External Validity: From Do-Calculus to Transportability Across Populations". In: *Stat. Sci.* (2014). URL: <http://arxiv.org/abs/1503.01603>.

Pedregosa, F. et al. "Scikit-learn: Machine Learning in Python". In: *Journal of Machine Learning Research* 12 (2011), pp. 2825–2830.

Peng, Xingchao et al. "Moment matching for multi-source domain adaptation". In: *Proceedings of the IEEE International Conference on Computer Vision*. 2019, pp. 1406–1415.

Puli, Aahlad Manas et al. "Out-of-distribution Generalization in the Presence of Nuisance-Induced Spurious Correlations". In: *ICLR*. May 2022. URL: <https://openreview.net/forum?id=12RoR2o32T>.

Renals, S et al. "Connectionist probability estimators in HMM speech recognition". In: *IEEE Trans. Audio Speech Lang. Processing* 2.1 (Jan. 1994), pp. 161–174. URL: <http://dx.doi.org/10.1109/89.260359>.

Saerens, Marco, Patrice Latinne, and Christine Daeaestecker. "Adjusting the Outputs of a Classifier to New a Priori Probabilities: A Simple Procedure". In: *Neural Computation* 14.1 (Jan. 2002), pp. 21–41. ISSN: 0899-7667. DOI: <10.1162/089976602753284446>. eprint: <https://direct.mit.edu/neco/article-pdf/14/1/21/815040/089976602753284446.pdf>. URL: <https://doi.org/10.1162/089976602753284446>.

Sagawa, Shiori et al. "Distributionally Robust Neural Networks for Group Shifts: On the Importance of Regularization for Worst-Case Generalization". In: *ICLR*. 2020. URL: <http://arxiv.org/abs/1911.08731>.

Schoelkopf, Bernhard et al. "On causal and anticausal learning". In: *Proceedings of the 29th International Conference on Machine Learning (ICML-12)*. Ed. by John Langford and Joelle Pineau. ICML '12. Edinburgh, Scotland, GB: Omnipress, July 2012, pp. 1255–1262. ISBN: 978-1-4503-1285-1. URL: <https://icml.cc/2012/papers/625.pdf>.

Sellergren, Andrew B et al. "Simplified Transfer Learning for Chest Radiography Models Using Less Data". In: *Radiology* 305.2 (Nov. 2022), pp. 454–465. URL: <http://dx.doi.org/10.1148/radiol.212482>.

Shu, Rui et al. "A DIRT-T Approach to Unsupervised Domain Adaptation". In: *International Conference on Learning Representations*. 2018. URL: <https://openreview.net/forum?id=H1q-TM-AW>.

Sohoni, Nimit S et al. "BARACK: Partially Supervised Group Robustness With Guarantees". In: (2021). arXiv: [2201.00072 \[cs.LG\]](2201.00072).

Tzeng, Eric et al. “Deep domain confusion: Maximizing for domain invariance”. In: *arXiv preprint arXiv:1412.3474* (2014).

Veitch, Victor et al. “Counterfactual Invariance to Spurious Correlations in Text Classification”. In: *NIPS*. Nov. 2021. URL: <https://openreview.net/forum?id=BdKxQp0iBi8>.

Wang, Dequan et al. “Tent: Fully Test-Time Adaptation by Entropy Minimization”. In: *International Conference on Learning Representations*. 2021. URL: <https://openreview.net/forum?id=uXl3bZLkr3c>.

Wang, Zihao and Victor Veitch. “A Unified Causal View of Domain Invariant Representation Learning”. In: (Aug. 2022). arXiv: [2208.06987 \[stat.ML\]](https://arxiv.org/abs/2208.06987). URL: <http://arxiv.org/abs/2208.06987>.

Wiles, Olivia et al. “A Fine-Grained Analysis on Distribution Shift”. In: *International Conference on Learning Representations*. 2022. URL: <https://openreview.net/forum?id=D14LetuLdyK>.

Zech, John R et al. “Variable generalization performance of a deep learning model to detect pneumonia in chest radiographs: A cross-sectional study”. en. In: *PLoS Med.* 15.11 (Nov. 2018), e1002683. URL: <http://dx.doi.org/10.1371/journal.pmed.1002683>.

Zhang, Kun et al. “Domain Adaptation under Target and Conditional Shift”. In: *ICML*. Vol. 28. 2013. URL: <http://proceedings.mlr.press/v28/zhang13d.pdf>.

Zhang, Marvin, Sergey Levine, and Chelsea Finn. “Memo: Test time robustness via adaptation and augmentation”. In: *arXiv preprint arXiv:2110.09506* (2021).

Zhang, Pan et al. “Prototypical pseudo label denoising and target structure learning for domain adaptive semantic segmentation”. In: *Proceedings of the IEEE/CVF conference on computer vision and pattern recognition*. 2021, pp. 12414–12424.

Zheng, Jiayun and Maggie Makar. “Causally motivated multi-shortcut identification and removal”. In: *NIPS*. Oct. 2022. URL: <https://openreview.net/forum?id=-ZQ0x6yaVa->.